

BFKL evolution and the growth with energy of exclusive J/Ψ and Υ photo-production cross-sections

I. Bautista¹, A. Fernandez Tellez¹ and M. Hentschinski^{1,2}

¹Facultad de Ciencias Físico Matemáticas,

Benemérita Universidad Autónoma de Puebla, Puebla 1152, Mexico

²Instituto de Ciencias Nucleares, Universidad Nacional Autónoma de México
Apartado Postal 70-543, Ciudad de México 04510, Mexico

November 17, 2016

Abstract

We investigate whether the Balitsky-Fadin-Kuraev-Lipatov (BFKL) low x evolution equation is capable to describe the energy dependence of the exclusive photo-production cross-section of vector mesons J/Ψ and Υ on protons. Such cross-sections have been measured by both HERA experiments H1 and ZEUS in electron-proton collisions and by LHC experiments ALICE, CMS and LHCb in ultra-peripheral proton-proton and ultra-peripheral proton-lead collisions. Our approach provides a perturbative description of the rise with energy and relies only on a fit of the initial transverse momentum profile of the proton impact factor, which can be extracted from BFKL fits to inclusive HERA data. We find that BFKL evolution is capable to provide a very good description of the energy dependence of the current data set, while the available fits of the proton impact factor require an adjustment in the overall normalization.

1 Introduction

The Large Hadron Collider (LHC) provides due to its large center of mass energy a unique opportunity to explore the high energy limit of Quantum Chromodynamics (QCD). In the presence of a hard scale the theoretical description of the latter is based on the Balitsky-Fadin-Kuraev-Lipatov (BFKL) evolution equation [1], currently known up to next-to-leading order (NLO) [2] in the strong coupling constant α_s . The bulk of searches for BFKL dynamics at the LHC concentrates on the analysis of correlations in azimuthal angles of jets, with the most prominent example the angular decorrelation of a pair of forward-backward or Mueller-Navelet jets. Data collected for such angular correlations during the 7 TeV run provide currently first phenomenological evidence for BFKL dynamics at the LHC [3]. More recent attempts on the theory side include now also the study of angular correlations of up to 4 jets, which are expected to provide further inside into BFKL dynamics and the realization of so-called Multi-Regge-Kinematics at the LHC [4].

The study of angular decorrelation is very attractive from a theory point of view, since the resulting perturbative description is very stable and only weakly affected by soft and

collinear radiative corrections. At the same time such angular decorrelations allow only to probe components of the BFKL kernel associated with non-zero conformal spin, $n \neq 0$. The exploration of $n \neq 0$ components is of interest in its own right and further allows already to test the calculational framework of high-energy factorization, which underlies the formulation of BFKL evolution. On the other hand these studies do not allow to address one of the central questions of the QCD high energy limit, namely the growth of perturbative cross-sections with energy. The latter corresponds to the so-called ‘hard’ Pomeron and is governed by the the conformal spin zero $n = 0$ component of the BFKL kernel.

Unlike the $n \neq 0$ terms, the $n = 0$ component is strongly affected by large (anti-) collinear logarithms which need to be resummed. Building on [5, 6], such a resummed NLO BFKL kernel has been constructed in [7, 8], and employed for a fit to proton structure functions measured in inclusive Deep Inelastic Scattering (DIS) at HERA. These results have then been subsequently used to extract an unintegrated gluon density and to provide predictions for rapidity and transverse momentum distributions of forward b -jets at the LHC in [9]. In the following we will study the cross-section for exclusive photo-production of vector mesons J/Ψ and Υ on a proton. In particular we are interested on a description of the rise with center-of-mass energy W of the $\gamma p \rightarrow Vp$ cross-section ($V = J/\Psi, \Upsilon$), combining measurements at HERA and the LHC. At the LHC the cross-sections for the process $\gamma p \rightarrow Vp$ can be extracted from ultra-peripheral proton-proton (pp) and proton-lead (pPb) collisions, which allow to test the gluon distribution in the proton down to very small values of the proton momentum fraction $x > 4 \cdot 10^{-6}$. For this processes the mass of the heavy quarks, *i.e.* charm (J/Ψ) and bottom (Υ), provide the hard mass-scale which allows for a description within perturbative QCD.

Currently there exist various studies of the data collected during the 7/8 TeV run [10–17], see also [18, 19]. In following we focus on the question whether perturbative BFKL evolution is capable to describe the rise of the $\gamma p \rightarrow Vp$ cross-section with energy *i.e.* we investigate whether the observed rise can be described purely perturbatively, avoiding both the use of a fitted W dependence as well as ideas related to gluon saturation. While our description involves necessarily also a fit of initial conditions to data, this fit is restricted to the transverse momentum distribution inside the proton, which has been determined in the analysis of HERA data in [7, 8]. The W -dependence arises on the other hand due to a solution of the NLO BFKL equation with collinear improvements, combined with an optimal renormalization scale setting.

The outline of this paper is as follows: In Sec. 2 we present the theoretical framework of our study, including a short review of the unintegrated BFKL gluon density of [9] and a determination of the vector meson photo-production impact factor. In Sec. 3 we present the numerical results of our study, including a comparison to data while we present in Sec. 4 our conclusions and an outlook on future work. Two integrals needed for the derivation of the impact factor are collected in the Appendix.

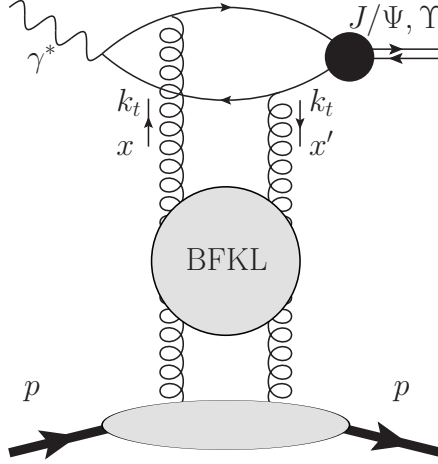


Figure 1: Schematic picture of the high energy factorized amplitude for photo-production of vector mesons $J/\Psi, \Upsilon$ with zero momentum transfer $t = 0$. In the high energy limit the amplitude factorizes into the impact factor for the transition $\gamma^* \rightarrow J/\Psi, \Upsilon$ (quark-loop), the BFKL-Green's function (central blob) and non-perturbative proton impact factor (lower blob).

2 Vector meson production in the high energy limit

In the following we describe the framework on which our study is based on. We study the process

$$\gamma(q) + p(p) \rightarrow V(q') + p(p'), \quad (1)$$

where $V = J/\Psi, \Upsilon(1S)$ while γ denotes a quasi-real photon with virtuality $Q \rightarrow 0$; $W^2 = (q + p)^2$ is the squared center-of-mass energy of the $\gamma(q) + p(p)$ collision. Neglecting proton mass effects, *i.e.* working in the limit $q^2 = 0 = p^2$, the following Sudakov decomposition holds for the final state momenta in the high energy limit $W \gg M_V$,

$$q' = q + \frac{M_V^2 + \Delta^2}{W^2} p + \Delta_t \quad p' = p + \frac{\Delta^2}{W^2} q - \Delta_t \quad (2)$$

with $l_t^2 = -l^2$ and $l_t \cdot p = 0 = l_t \cdot q$ for a generic momentum l . With the momentum transfer $t = (q - q')^2 = -\Delta^2$, the differential cross-section for the exclusive production of a vector meson can be written in the following form

$$\frac{d\sigma}{dt} (\gamma p \rightarrow V p) = \frac{1}{16\pi} \left| \mathcal{A}_{T,L}^{\gamma p \rightarrow V p}(W^2, t) \right|^2. \quad (3)$$

where $\mathcal{A}(W^2, t)$ denotes the scattering amplitude for the reaction $\gamma p \rightarrow V p$ for color singlet exchange in the t -channel, with an overall factor W^2 already extracted. Within high energy factorization *i.e.* discarding terms $\sim M_V^2/W^2$, this scattering amplitude can be written as a convolution in transverse momentum space of the universal BFKL Green's-function, which achieves a resummation of high energy logarithms $\ln W^2$ to all orders in the strong coupling constant α_s , and two process-dependent impact factors which describe the coupling of the Green's function to external states, see Fig. 1. In the present case, one of the impact factors

	virt. photon impact factor	Q_0/GeV	δ	\mathcal{C}
fit 1	leading order (LO)	0.28	8.4	1.50
fit 2	LO with kinematic improvements	0.28	6.5	2.35

Table 1: Parameters of the proton impact factor obtained in [8] through a fit to combined HERA data

describes the transition $\gamma \rightarrow V$ and is characterized by the heavy quark mass m_c and m_b respectively, which provide the hard scale of the process. The second impact factor, which describes the transition $p \rightarrow p$ is of non-perturbative origin; it needs to be modeled with free parameters to be fixed by a fit to data.

In the high energy limit $W^2 \gg M_V^2$, this scattering amplitude is dominated by its imaginary part, $\mathcal{A}(W^2, t) \simeq i \cdot \text{Im} \mathcal{A}(W^2, t)$, with the real part suppressed by powers of α_s . Limiting ourselves for the moment to the dominant imaginary part we find that for the case of zero momentum transfer, $t = -\Delta^2 = 0$, the non-perturbative proton impact factor coincides for this process with the corresponding proton impact factor found in fits to Deep-Inelastic Scattering data. Such a fit of the forward $t = 0$ proton impact factor has been performed in [7, 8] which can be therefore used for phenomenological studies of vector meson production.

2.1 The NLO collinear improved BFKL unintegrated gluon density

In [7, 8] the following model has been used for the proton impact factor

$$\Phi_p \left(\frac{\mathbf{q}^2}{Q_0^2}, \delta \right) = \frac{\mathcal{C}}{\pi \Gamma(\delta)} \left(\frac{\mathbf{q}^2}{Q_0^2} \right)^\delta e^{-\frac{\mathbf{q}^2}{Q_0^2}}. \quad (4)$$

The model introduces 2 free parameters plus an overall normalization factor and provides a Poisson-distribution peaked at $\mathbf{q}^2 = \delta Q_0^2$. Depending on the precise form of the virtual photon impact factor, two sets of parameters have been determined, which are summarized in Tab. 1, where for the second fit the leading order virtual photon impact factor has been supplemented with DGLAP inspired kinematic corrections [20]; both fits have been performed for $n_f = 4$ mass-less flavors.

In [9] the results of this fit have been used to introduce a NLL BFKL unintegrated gluon density as the following convolution of proton impact factor and BFKL Green's function

$$G(x, \mathbf{k}^2, Q_0^2) = \int \frac{d\mathbf{q}^2}{\mathbf{q}^2} \mathcal{F}^{\text{DIS}}(x, \mathbf{k}^2, \mathbf{q}^2) \Phi_p \left(\frac{\mathbf{q}^2}{Q_0^2} \right). \quad (5)$$

In Mellin space conjugate to transverse momentum space this unintegrated gluon density can be written as

$$G(x, \mathbf{k}^2, M) = \frac{1}{\mathbf{k}^2} \int_{\frac{1}{2}-i\infty}^{\frac{1}{2}+i\infty} \frac{d\gamma}{2\pi i} \hat{g} \left(x, \frac{M^2}{Q_0^2}, \frac{\overline{M}^2}{M^2}, \gamma \right) \left(\frac{\mathbf{k}^2}{Q_0^2} \right)^\gamma \quad (6)$$

where M is a characteristic hard scale of the process which in the case of the DIS fit has been identified with the virtuality of the photon and \bar{M} is a corresponding scale which enters the running coupling constant (see also the discussion below); in the DIS analysis $M = \bar{M}$ and both scales have been identified with the virtuality of the scattering photon. \hat{g} is finally an operator in γ space and defined as

$$\hat{g}\left(x, \frac{M^2}{Q_0^2}, \frac{\bar{M}^2}{M^2}, \gamma\right) = \frac{\mathcal{C} \cdot \Gamma(\delta - \gamma)}{\pi \Gamma(\delta)} \cdot \left(\frac{1}{x}\right)^{\chi\left(\gamma, \frac{\bar{M}^2}{M^2}\right)} \cdot \left\{ 1 + \frac{\bar{\alpha}_s^2 \beta_0 \chi_0(\gamma)}{8N_c} \log\left(\frac{1}{x}\right) \left[-\psi(\delta - \gamma) + \log\frac{M^2}{Q_0^2} - \partial_\gamma \right] \right\}, \quad (7)$$

where $\bar{\alpha}_s = \alpha_s N_c / \pi$ with N_c the number of colors and $\chi(\gamma, \bar{M}^2/M^2)$ is the next-to-leading logarithmic (NLL) BFKL kernel after collinear improvements; in addition large terms proportional to the first coefficient of the QCD beta function, $\beta_0 = 11N_c/3 - 2n_f/3$ have been resummed through employing a Brodsky-Lepage-Mackenzie (BLM) optimal scale setting scheme [21]. The NLL kernel with collinear improvements reads

$$\chi\left(\gamma, \frac{\bar{M}^2}{M^2}\right) = \bar{\alpha}_s \chi_0(\gamma) + \bar{\alpha}_s^2 \tilde{\chi}_1(\gamma) - \frac{1}{2} \bar{\alpha}_s^2 \chi_0'(\gamma) \chi_0(\gamma) + \chi_{RG}(\bar{\alpha}_s, \gamma, \tilde{a}, \tilde{b}) - \frac{\bar{\alpha}_s^2 \beta_0}{8N_c} \chi_0(\gamma) \log\frac{\bar{M}^2}{M^2}. \quad (8)$$

with the leading-order BFKL eigenvalue,

$$\chi_0(\gamma) = 2\psi(1) - \psi(\gamma) - \psi(1 - \gamma). \quad (9)$$

We note that the last term in the second line of Eq. (8) was not present in the final results of [7, 8] and [9], but can be easily derived from an intermediate result provided in [7]. It has been re-introduced to assess possible uncertainties of the final result due to identifying $\bar{M} = M$. The term responsible for the resummation of collinear enhanced terms reads

$$\chi_{RG}(\bar{\alpha}_s, \gamma, a, b) = \bar{\alpha}_s (1 + a\bar{\alpha}_s) (\psi(\gamma) - \psi(\gamma - b\bar{\alpha}_s)) - \frac{\bar{\alpha}_s^2}{2} \psi''(1 - \gamma) - \frac{b\bar{\alpha}_s^2 \cdot \pi^2}{\sin^2(\pi\gamma)} + \frac{1}{2} \sum_{m=0}^{\infty} \left(\gamma - 1 - m + b\bar{\alpha}_s - \frac{2\bar{\alpha}_s(1 + a\bar{\alpha}_s)}{1 - \gamma + m} + \sqrt{(\gamma - 1 - m + b\bar{\alpha}_s)^2 + 4\bar{\alpha}_s(1 + a\bar{\alpha}_s)} \right). \quad (10)$$

For details on the derivation of this term we refer to the discussion in [7], see also [5, 6]. Employing BLM optimal scale setting and the momentum space (MOM) physical renormalization scheme based on a symmetric triple gluon vertex [22] with $Y \simeq 2.343907$ and gauge

parameter $\xi = 3$ one obtains the following next-to-leading order BFKL eigenvalue

$$\begin{aligned}\tilde{\chi}_1(\gamma) &= \tilde{\mathcal{S}}\chi_0(\gamma) + \frac{3}{2}\zeta(3) + \frac{\Psi''(\gamma) + \Psi''(1-\gamma) - \phi(\gamma) - \phi(1-\gamma)}{4} \\ &\quad - \frac{\pi^2 \cos(\pi\gamma)}{4 \sin^2(\pi\gamma)(1-2\gamma)} \left[3 + \left(1 + \frac{n_f}{N_c^3} \right) \frac{2 + 3\gamma(1-\gamma)}{(3-2\gamma)(1+2\gamma)} \right] \\ &\quad + \frac{1}{8} \left[\frac{3}{2}(Y-1)\xi + \left(1 - \frac{Y}{3} \right) \xi^2 + \frac{17Y}{2} - \frac{\xi^3}{6} \right] \chi_0(\gamma),\end{aligned}\tag{11}$$

where $\tilde{\mathcal{S}} = \frac{(4-\pi^2)}{12}$, see also the discussion in [23]. The coefficients \tilde{a}, \tilde{b} which enter the collinear resummation term Eq. (10) are obtained as the coefficients of the $1/\gamma$ and $1/\gamma^2$ poles of the NLO eigenvalue. In the case of Eq. (11) one has

$$\begin{aligned}\tilde{a} &= -\frac{13}{36} \frac{n_f}{N_c^3} - \frac{55}{36} + \frac{3Y-3}{16} \xi + \frac{3-Y}{24} \xi^2 - \frac{1}{48} \xi^3 + \frac{17}{16} Y \\ \tilde{b} &= -\frac{n_f}{6N_c^3} - \frac{11}{12}.\end{aligned}\tag{12}$$

Employing BLM optimal scale setting, the running coupling constant becomes dependent on the Mellin-variable γ and reads

$$\tilde{\alpha}_s(\bar{M} \cdot Q_0, \gamma) = \frac{4N_c}{\beta_0 \left[\log\left(\frac{\bar{M} \cdot Q_0}{\Lambda^2}\right) + \frac{1}{2}\chi_0(\gamma) - \frac{5}{3} + 2\left(1 + \frac{2}{3}Y\right) \right]},\tag{13}$$

In addition, in order to access the region of small photon virtualities, in [7, 8], a parametrization of the running coupling introduced by Webber in Ref. [24] has been used,

$$\alpha_s(\mu^2) = \frac{4\pi}{\beta_0 \ln \frac{\mu^2}{\Lambda^2}} + f\left(\frac{\mu^2}{\Lambda^2}\right), \quad f\left(\frac{\mu^2}{\Lambda^2}\right) = \frac{4\pi}{\beta_0} \frac{125 \left(1 + 4\frac{\mu^2}{\Lambda^2}\right)}{\left(1 - \frac{\mu^2}{\Lambda^2}\right) \left(4 + \frac{\mu^2}{\Lambda^2}\right)^4},\tag{14}$$

with $\Lambda = 0.21$ GeV. At low scales this modified running coupling is consistent with global data of power corrections to perturbative observables, while for larger values it coincides with the conventional perturbative running coupling constant. For further details we refer the interested reader to [7, 8] and references therein.

2.2 The vector meson photo-production impact factor

To use the above unintegrated gluon density for the description of the process $\gamma p \rightarrow Vp$, we still require the impact factor for the transition $\gamma \rightarrow V$. To the best of our knowledge, such an impact factor is currently not known within the BFKL framework. It is however possible to extract the required quantity from a description based on a factorization of the amplitude in the high energy limit into light-front wave function and dipole amplitude. In the dilute limit, the factorization into light-front wave function and dipole amplitude becomes equivalent to the factorization into impact factor and unintegrated gluon density and it is therefore possible to recover the required impact factor from these results. Our starting

Meson	m_f/GeV	\mathcal{N}_T	$\mathcal{R}^2/\text{GeV}^{-2}$	M_V/GeV	$8\mathcal{R}^{-\epsilon}/\text{GeV}^2$	$\frac{1}{4}M_V^2/\text{GeV}^2$
J/ψ	$m_c = 1.27$	0.596	2.45	3.097	3.27	2.40
Υ	$m_b = 4.2$	0.481	0.57	9.460	15.38	22.42

Table 2: Parameters of the boosted Gaussian vector meson wave functions for J/ψ and Υ obtained in [14, 16]. The last two columns give the two possible hard scales used in the BFKL analysis.

point is the following expression for the imaginary part of the vector meson photo-production scattering amplitude [25, 26]

$$\Im \mathcal{A}_{T,L}^{\gamma^* p \rightarrow V p}(W, t) = 2 \int d^2\mathbf{r} \int d^2\mathbf{b} \int_0^1 \frac{dz}{4\pi} (\Psi_V^* \Psi)_{T,L} e^{-i[\mathbf{b} - (1-z)\mathbf{r}] \cdot \mathbf{\Delta}} \mathcal{N}(x, r, b), \quad (15)$$

where $\mathcal{N}(x, r, b)$ is the dipole amplitude and T, L denotes transverse and longitudinal polarization of the virtual photon respectively and $t = -\mathbf{\Delta}^2$. The overlap between the photon and the vector meson light-front wave function reads

$$\begin{aligned} (\Psi_V^* \Psi)_T(r) &= \hat{e}_f e \frac{N_c}{\pi z(1-z)} \left\{ m_f^2 K_0(\epsilon r) \phi_T(r, z) - [z^2 + (1-z)^2] \epsilon K_1(\epsilon r) \partial_r \phi_T(r, z) \right\} \\ (\Psi_V^* \Psi)_L(r) &= \hat{e}_f e \frac{N_c}{\pi} 2Qz(1-z) K_0(\epsilon r) \left\{ M_V \phi_L(r, z) + \delta \frac{m_f^2 - \nabla_r^2}{M_V z(1-z)} \phi_L(r, z) \right\}, \end{aligned} \quad (16)$$

where from now on we discard longitudinal photon polarizations since the corresponding wave function overlap is vanishing in the limit $Q \rightarrow 0$ in which we are working. To keep our result applicable to the case $Q \neq 0$, we however keep on using the notation $\epsilon^2 \equiv z(1-z)Q^2 + m_f^2$, with $\epsilon^2 = m_f^2$ for real photons. Furthermore $r = \sqrt{\mathbf{r}^2}$, while $f = c, b$ denotes the flavor of the heavy quark, with charge $\hat{e}_f = 2/3, 1/3$, corresponding to J/ψ and Υ mesons respectively. For the scalar parts of the wave functions $\phi_{T,L}(r, z)$, we follow closely [14] and employ the boosted Gaussian wave-functions with the Brodsky-Huang-Lepage prescription [27]. For the ground state vector meson ($1s$) the scalar function $\phi_{T,L}(r, z)$, has the following general form [26, 28],

$$\phi_{T,L}^{1s}(r, z) = \mathcal{N}_{T,L} z(1-z) \exp \left(-\frac{m_f^2 \mathcal{R}_{1s}^2}{8z(1-z)} - \frac{2z(1-z)r^2}{\mathcal{R}_{1s}^2} + \frac{m_f^2 \mathcal{R}_{1s}^2}{2} \right). \quad (17)$$

The free parameters N_T and \mathcal{R}_{1s} of this model have been determined in various studies from the normalization condition of the wave function and the decay width of the vector mesons. In the following we use the most recent available values *i.e.* [14] (for the J/Ψ) and [16] (for the Υ) The results are summarized in Tab. 2. In the forward limit $t = 0$, the entire dependence of the integrand on the impact parameter \mathbf{b} is contained in the dipole amplitude which results into the following inclusive dipole cross-section,

$$2 \int d^2\mathbf{b} \mathcal{N}(x, r, b) = \sigma_0 N(x, \mathbf{r}). \quad (18)$$

The relation between the latter and an unintegrated gluon density has been worked in [29] and is given by

$$\sigma_0 N(\mathbf{r}, x) = \frac{4\pi}{N_c} \int \frac{d^2\mathbf{k}}{\mathbf{k}^2} \left(1 - e^{i\mathbf{k} \cdot \mathbf{r}}\right) \alpha_s G(x, \mathbf{k}^2). \quad (19)$$

This expression can then be used to calculate the BFKL impact factor from the light-front wave function overlap Eq. (16). In particular we find

$$\begin{aligned} \Im \mathcal{A}_T^{\gamma^* p \rightarrow V p}(W, 0) &= \int d^2 \mathbf{r} \int_0^1 \frac{dz}{4\pi} (\Psi_V^* \Psi)_T(r) \cdot \sigma_0 N(x, r) \\ &= \alpha_s (\overline{M} \cdot Q_0) \int_{\frac{1}{2}-i\infty}^{\frac{1}{2}+i\infty} \frac{d\gamma}{2\pi i} \int_0^1 \frac{dz}{4\pi} \hat{g} \left(x, \frac{M^2}{Q_0^2}, \frac{\overline{M}^2}{M^2}, Q_0, \gamma \right) \cdot \Phi_{V,T}(\gamma, z, M) \cdot \left(\frac{M^2}{Q_0^2} \right)^\gamma. \end{aligned} \quad (20)$$

In the above expression, M and \overline{M} are the mass-scales introduced in Eq. (7). The scale of the strong coupling α_s in Eq. (19), (20) has been set in accordance with the conventions used in the HERA fit¹ [8]. From Eq. (20) we obtain

$$\begin{aligned} \Phi_{V,T}(\gamma, z, M) &= \frac{4\pi}{N_c} \int d^2 \mathbf{r} \int \frac{d^2 \mathbf{k}}{(\mathbf{k}^2)^2} (1 - e^{i\mathbf{k} \cdot \mathbf{r}}) \left(\frac{\mathbf{k}^2}{M^2} \right)^\gamma (\Psi_V^* \Psi)_T(r) \\ &= e \hat{e}_f 8\pi^2 \mathcal{N}_T \frac{\Gamma(\gamma)\Gamma(1-\gamma)}{m_f^2} \left(\frac{m_f^2 \mathcal{R}^2}{8z(1-z)} \right)^2 e^{-\frac{m_f^2 \mathcal{R}^2}{8z(1-z)}} e^{\frac{m_f^2 \mathcal{R}^2}{2}} \left(\frac{8z(1-z)}{M^2 \mathcal{R}^2} \right)^\gamma \\ &\quad \left[U \left(2-\gamma, 1, \frac{\epsilon^2 \mathcal{R}^2}{8z(1-z)} \right) + [z^2 + (1-z)^2] \frac{\epsilon^2 (2-\gamma)}{2 \cdot m_f^2} U \left(3-\gamma, 2, \frac{\epsilon^2 \mathcal{R}^2}{8z(1-z)} \right) \right], \end{aligned} \quad (21)$$

where $U(a, b, z)$ is a hypergeometric function of the second kind or Kummer's function. Some useful integrals in the derivation of this result are summarized in the appendix. Expanding Eq. (20) to NLO in α_s , it is straightforward to verify that our result is independent of M to NLO accuracy. Furthermore one can verify that the resummed BFKL eigenvalue Eq. (8) is furthermore independent of the choice of \overline{M} up to terms $\mathcal{O}(\alpha_s^3)$.

2.3 Real part, phenomenological corrections and integrated cross-sections

Even though the real part of the scattering amplitude is suppressed by powers of α_s in the high energy limit, it can still provide a sizable correction to the cross-section and should be therefore included. In the high energy limit it is possible to obtain this real part from the imaginary part using dispersion relation. One has

$$\frac{\Re \mathcal{A}(W^2, t)}{\Im \mathcal{A}(W^2, t)} = \tan \frac{\lambda \pi}{2}, \quad \text{with} \quad \lambda = \frac{d \ln \mathcal{A}(W^2, t)}{d \ln W^2}. \quad (22)$$

Eq. (22) is frequently used in the literature in the study of photo-production of vector mesons. Within our framework we write first the imaginary part of the scattering amplitude as a

¹A precise determination of the scale of this running coupling would require the complete NLO corrections to the impact factor which are currently not available

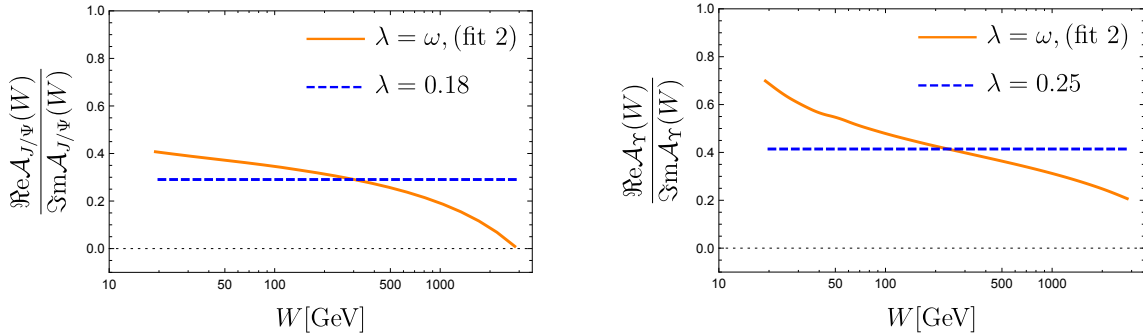


Figure 2: Ratio of real and imaginary part of the $\gamma p \rightarrow Vp$ scattering amplitude for $V = J/\Psi$ (left) and $V = \Upsilon$ (right) as obtained from using a constant value (dashed) for λ in Eq. (22) and the identification $\lambda = \omega$, see Eq. (23) and the subsequent discussion (continuous).

double Mellin transform

$$\begin{aligned} \Im \mathcal{A}_T^{\gamma p \rightarrow Vp}(W^2, 0) &= \alpha_s(\overline{M} \cdot Q_0) \cdot \int_{\delta-i\infty}^{\delta+i\infty} \frac{d\omega}{2\pi i} \left(\frac{1}{x}\right)^\omega \int_{\frac{1}{2}-i\infty}^{\frac{1}{2}+i\infty} \frac{d\gamma}{2\pi i} \left(\frac{M^2}{Q_0^2}\right)^\gamma \\ &\int_0^1 \frac{dz}{4\pi} \Phi_{V,T}(\gamma, z, M) \frac{\mathcal{C} \cdot \Gamma(\delta - \gamma)}{\pi \Gamma(\delta)} \cdot \left\{ \frac{1}{\omega - \chi\left(\gamma, \frac{M^2}{M^2}\right)} \right. \\ &\left. + \frac{\bar{\alpha}_s^2 \beta_0 \chi_0(\gamma)/(8N_c)}{\left[\omega - \chi\left(\gamma, \frac{M^2}{M^2}\right)\right]^2} \left[-\psi(\delta - \gamma) - \frac{d \ln [\Phi_{V,T}(\gamma, z, M)]}{d\gamma} \right] \right\}, \quad (23) \end{aligned}$$

where the ω -contour runs to the right of all singularities and $x = \frac{M_V^2}{W^2 - m_p^2}$, with $m_p = .938$ GeV the proton mass; note that $\mathcal{A}_L = 0$ due to $Q = 0$. To determine the real part we identify λ with the Mellin variable conjugate to the x , $\lambda = \omega$. The complete amplitude is then obtained through multiplying the integrand of Eq. (23) by a factor $(i + \tan \frac{\omega\pi}{2})$. The Mellin transform w.r.t. ω is then easily evaluated through taking residues at the single and double pole at $\omega = \chi(\gamma, \overline{M}^2 \cdot M^2)$, while residues at $\omega = -1, -3, \dots$ are subleading in the high energy/low x limit and therefore neglected. As a consequence we obtain – in contrast to the bulk of phenomenological studies in the literature – an energy dependent ratio of real and imaginary part, see Fig. 2 for numerical results. Particular for small values of W , the real part provides a relative large correction, up to 41% in the case of the J/Ψ and 70% in the case of the Υ , see also the discussion in [30]. On the other hand, since this ratio is decreasing with increasing W , we find that this energy-dependent ratio leads to a slow-down of the growth with energy in the high energy region.

Another phenomenological correction to the cross-section, which is often included in studies of vector meson photo-production, arises due to the fact that the proton momentum fractions x, x' of the two gluons coupling to the $\gamma \rightarrow V$ transition, can differ, even though we are working in the forward limit $t = 0$. In [31] a corresponding corrective factor has been determined for the case of the conventional (integrated) gluon distribution, by relating the

latter through a Shuvaev transform to the generalized parton distribution (GPD). Since we are dealing in the current case with an transverse momentum dependent (unintegrated) gluon density, such a corrective factor would at best be correct approximately. Our numerical studies find no significant improvement in the description of data due to such a factor and we therefore do not include it in our analysis.

While we calculated so far the differential cross-section at momentum transfer $t = 0$, experimental data which we wish to analyze, are usually given for cross-sections integrated over t . It is therefore necessary to model the t -dependence and to relate in this way the differential cross-section at $t = 0$ to the integrated cross-section. Here we follow the prescription given in [10, 11], who assume an exponential drop-off with $|t|$, $\sigma \sim \exp[-|t|B_D(W)]$ with an energy dependent t slope parameter B_D , which can be motivated by Regge theory,

$$B_D(W) = \left[b_0 + 4\alpha' \ln \frac{W}{W_0} \right] \text{GeV}^{-2}. \quad (24)$$

For the numerical values we use $\alpha' = 0.06 \text{ GeV}^{-2}$, $W_0 = 90 \text{ GeV}$ and $b_0^{J/\Psi} = 4.9 \text{ GeV}^{-2}$ in the case of the J/Ψ , while $b_0^\Upsilon = 4.63 \text{ GeV}^{-2}$ for Υ production, as proposed in [10, 11]. The total cross-section for vector meson production is therefore obtained as

$$\sigma^{\gamma p \rightarrow Vp}(W^2) = \frac{1}{B_D(W)} \frac{d\sigma}{dt} (\gamma p \rightarrow Vp) \Big|_{t=0}. \quad (25)$$

For the sake of completeness we further provide our final expression for the differential cross-section at $t = 0$. It is given by Eq. (3) for the case $t = 0$ with

$$\begin{aligned} \mathcal{A}_T^{\gamma p \rightarrow Vp}(W^2, 0) &= \alpha_s(\bar{M} \cdot Q_0) \cdot \int_{\frac{1}{2}-i\infty}^{\frac{1}{2}+i\infty} \frac{d\gamma}{2\pi i} \left(\frac{M^2}{Q_0^2} \right)^\gamma \left(i + \tan \frac{\pi \cdot \chi(\gamma, \frac{\bar{M}^2}{M^2})}{2} \right) \\ &\int_0^1 \frac{dz}{4\pi} \Phi_{V,T}(\gamma, z, M) \frac{\mathcal{C} \cdot \Gamma(\delta - \gamma)}{\pi \Gamma(\delta)} \cdot \left(\frac{1}{x} \right)^{\chi(\gamma, \frac{\bar{M}^2}{M^2})} \cdot \left\{ 1 + \frac{\bar{\alpha}_s^2 \beta_0 \chi_0(\gamma)}{8N_c} \left[\ln \left(\frac{1}{x} \right) \right. \right. \\ &\left. \left. + \frac{\pi}{2} \left(\tan \left[\frac{\pi \chi \left(\gamma, \frac{\bar{M}^2}{M^2} \right)}{2} \right] - i \right) \right] \left[-\psi(\delta - \gamma) - \frac{d \ln [\Phi_{V,T}(\gamma, z, M)]}{d\gamma} \right] \right\}, \quad (26) \end{aligned}$$

where $x = \frac{M_V^2}{W^2 - m_p^2}$.

3 Numerical results and Discussion

Our results for the W -dependence of the total $\gamma p \rightarrow Vp$ cross-section are depicted in Fig. 3 (J/Ψ) and Fig. 4 (Υ) and compared to data from HERA and LHC experiments. Both fits of free parameters of the proton impact factor, summarized in Tab. 1, are shown in the plots. We further show results for two different choices of the ‘hard’ scale M^2 of the unintegrated gluon density, *i.e.* the photoproduction scale $M^2 = M_V^2/4$ and the scale $M^2 = 8/\mathcal{R}^2$, see Tab. 2 for numerical values. The choice $M^2 = 8/\mathcal{R}^2$ is motivated by the structure of the

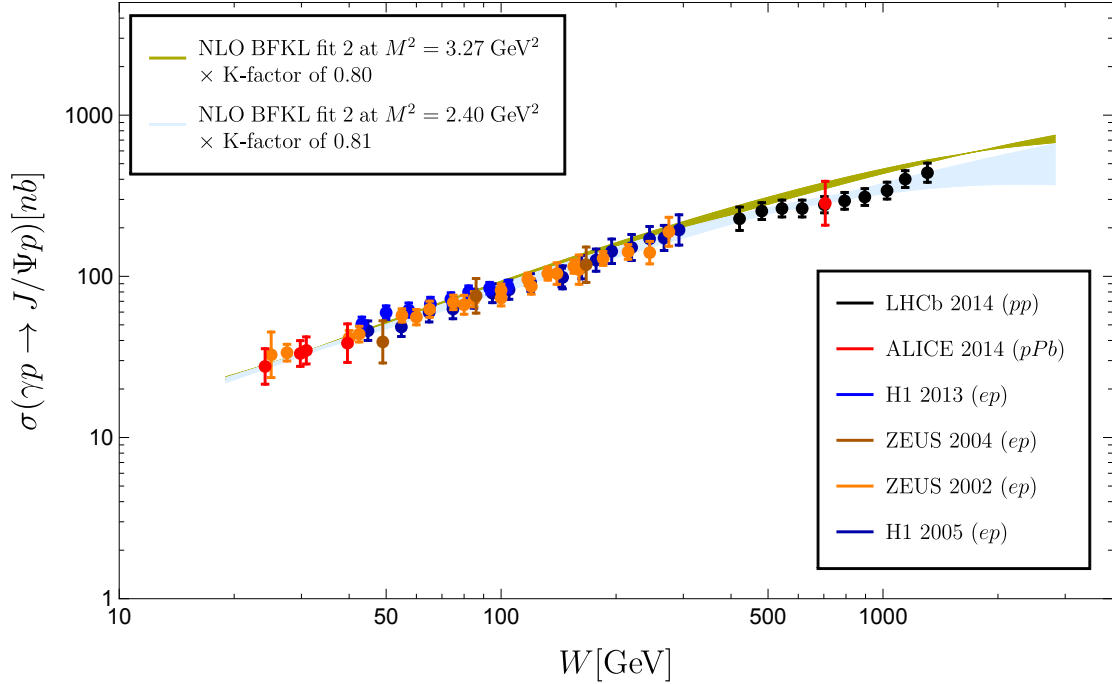
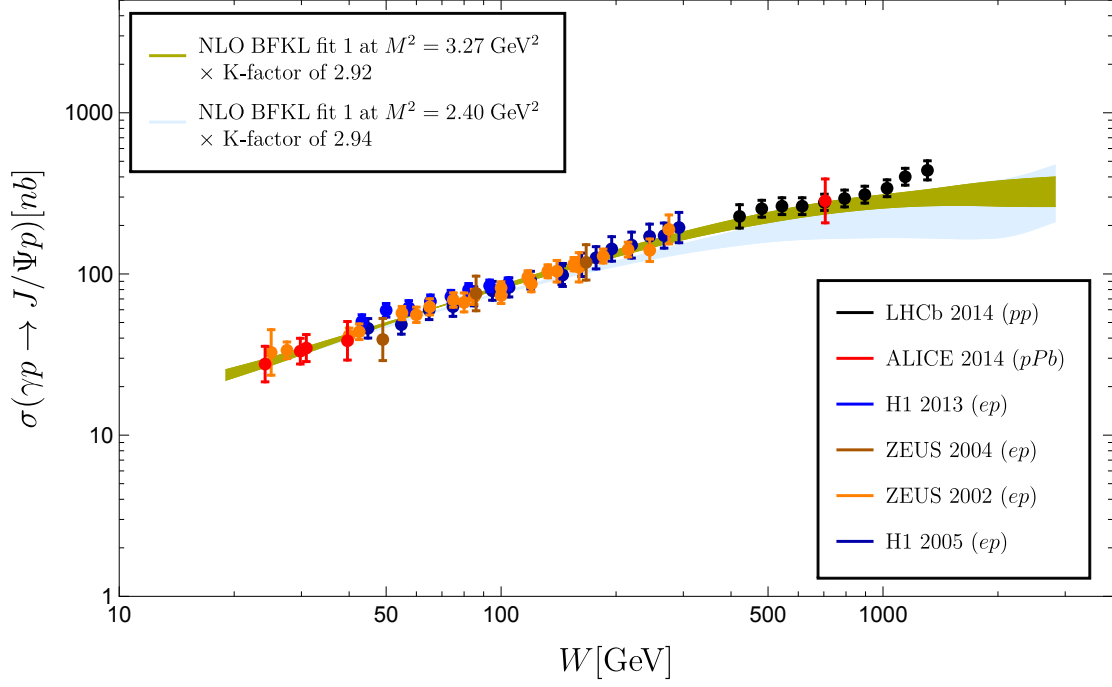


Figure 3: Energy dependence of the J/Ψ photo-production cross-section as provided by the BFKL fit 1 (up) and 2 (down). The uncertainty band reflects a variation of the scale $\bar{M}^2 \rightarrow \{\bar{M}^2/2, \bar{M}^2 \cdot 2\}$. We also show photo-production data measured at HERA by ZEUS [32, 33] and H1 [34, 35] as well as LHC data obtained from ALICE [36] and LHCb (W^+ solutions) [37].

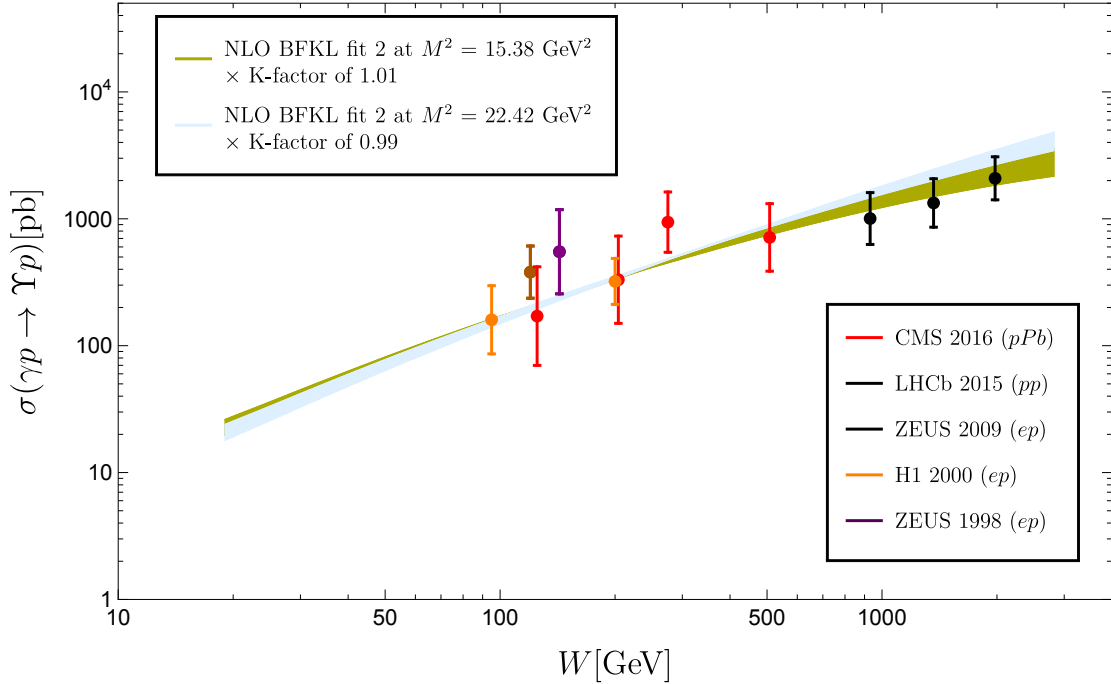
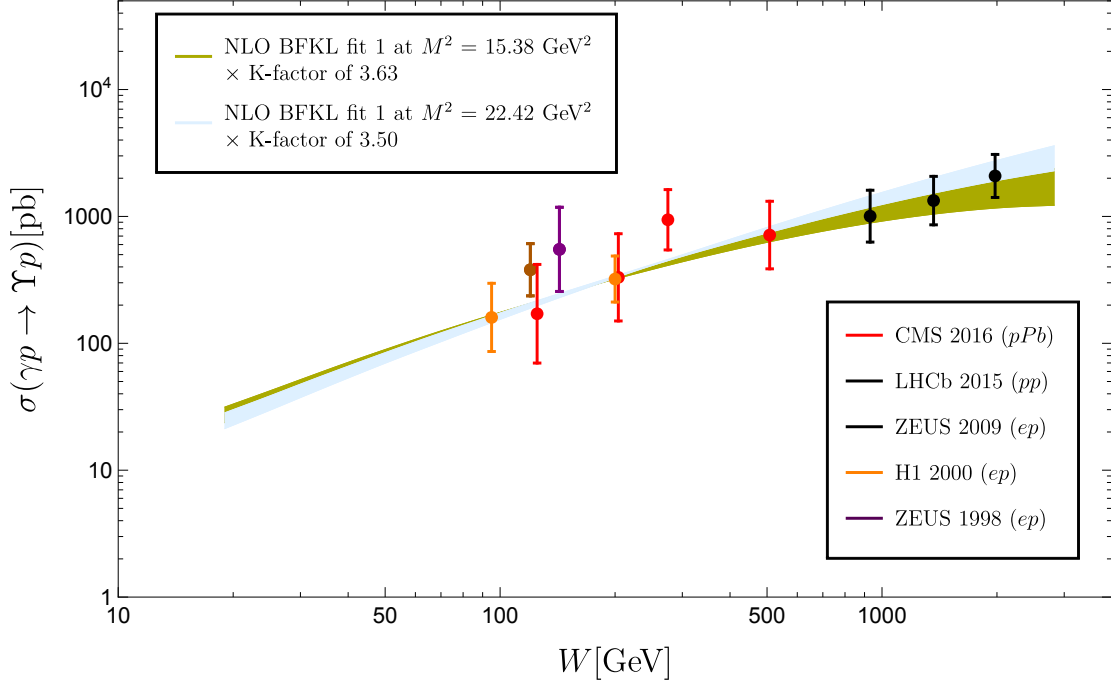


Figure 4: Energy dependence of the Υ photo-production cross-section as provided by the BFKL fit 1 (up) and 2 (down). The uncertainty band reflects a variation of the scale $\bar{M}^2 \rightarrow \{\bar{M}^2/2, \bar{M}^2 \cdot 2\}$. We also show HERA data measured by H1 [38] and ZEUS [39, 40] and LHC data by LHCb [41] and CMS [42].

impact factor Eq. (21), where it cancels the (z -independent part) of the factor $(..)^{\gamma}$ and therefore removes the scale dependence²; we further find that this choice seems to minimize the size of the term $d \ln \Phi_{V,T}/d\gamma$ in Eq. (26). We find that our result is only mildly dependent on this choice. Since the effective Pomeron intercept increases with increasing hard scale, see also [7, 8], the observed rise is always slightly stronger for the larger of the two scales. We further identify $\overline{M} = M$, while we vary \overline{M}^2 in the interval $[M^2/2, 2M^2]$ to assess the uncertainty associated with this choice. We find that the result is rather stable under this variation.

Comparing our results with data we find that the overall normalization obtained from the combination of BFKL gluon density and $\gamma \rightarrow V$ impact factor does – for the majority of cases – not coincide with measured data. This is in particular true for the BFKL fit 1, where typical values of necessary K -factors lie in the range 3 – 3.5. The BFKL fit 2 requires on the other hand only a small (0.80 – 0.81 for J/Ψ) or no correction (0.99 – 1.01 for Υ). In the current analysis we fix this normalization by the central values of some arbitrarily picked low energy data points, *i.e.* low energy ALICE (J/Ψ) and ZEUS (Υ) data. While it is possible to improve further the description through fitting the normalization to the entire data set, we believe that the current treatment is best suited to study the description of the W -dependence, on which we focus here.

Turning to the W -dependence we find that both fits and both scale choices allow for an excellent description of data in the case of Υ -production, see Fig. 4, where fit 2 essentially requires no K -factor. For the J/Ψ data set we find that fit 2 provides a very good description of the data (with a K -factor ~ 0.8 of order one), revealing a slight preference for the photoproduction scale $M^2 = M_{J/\Psi}^2/4$. The BFKL description based on the fit 1 also allows for a very good description of the W -dependence up to the last 2 LHCb data points, for which the predicted growth with W is too slow. Despite of this slight mismatch of fit 1 in the case of J/Ψ production, we find that the observed agreement with data is remarkable. This is in particular true for data points with $W > 500$ GeV which require x -evolution beyond the region constrained by the fit to HERA data and for which the obtained description directly tests the validity of the present implementation of NLO BFKL evolution.

While the observed mismatch in the overall normalization is not completely satisfactory, it is somehow expected and – at least for the BFKL fit 2 where the correction is small – easily explained by the limitations of the current framework. In the case of fit 1 a first improvement is obtained if corrections due to $x \neq x'$ (as available for the collinear gluon distribution function as discussed in Sec. 2.3) are included. Nevertheless also these corrections are not capable to account for the complete K -factor. For fit 2 one has to take into account that this fit is based on a leading order virtual photon impact factor with kinematic improvements [20], while the currently used impact factor for the transition $\gamma \rightarrow V$ does not contain such kinematic improvements; in the case of $\gamma \rightarrow V$ such corrections would also include corrections due to $x \neq x'$. While the kinematic improvements reduce in the case of DIS studies the magnitude of the impact factors, corrections due to $x \neq x'$ are for the case of vector mesons known to enhance the impact factor, at least in the collinear limit. In the case of fit 2

²The impact factor is of course still dependent on ratios of other scales. This is natural since, unlike the inclusive DIS impact factor, it is not characterized by a single hard scale.

we therefore expect to a large extent a cancellation of both effects. A second point which applies both to fit 1 and fit 2 is concerned with the treatment of heavy quark masses: while the impact factor Eq. (21) obviously depends on the heavy quark mass, the original DIS fits are limited to $n_f = 4$ mass-less flavors. Altogether we believe that it is more than plausible that such effects can account for the observed mismatch in normalization, in particular in the case of fit 2 where the mismatch is rather mild.

4 Outlook and Conclusions

In this work we applied the inclusive BFKL fit of [8] to the description of exclusive vector meson photo-production at HERA and the LHC. As a new result we calculated the impact factor for the $\gamma \rightarrow V$ transition in the γ -Mellin space representation, using earlier result based on the light-front wave function of vector mesons used in the combination with color dipole models. Our phenomenological studies show that the BFKL fits of [8] can provide a very good description of the center-of-mass energy dependence of the $\gamma p \rightarrow J/\Psi p$ and $\gamma p \rightarrow \Upsilon p$ cross-sections. While the BFKL fit 1 requires a relatively large adjustment in the overall normalization (of order 3 – 3.5), the necessary adjustment is of order one in the case of BFKL fit 2. We stress that the current analysis uses only a fit of the transverse momentum distribution in the proton, while the W -dependence directly results from NLO BFKL resummation, together with a resummation of collinearly enhanced terms within the NLO kernel and a optimal renormalization scale setting for the scale invariant terms of the NLO BFKL kernel. The study provides therefore direct evidence for the validity of BFKL evolution at the LHC.

Despite of the success of the current description, there are a number of directions in which our analysis could and should be re-fined. This implies at first the determination of kinematic corrections to the impact factor for the transition $\gamma \rightarrow V$, which might provide an opportunity to improve on the observed mismatch in the overall normalization. To improve the description further, it will be necessary to provide a re-fit of HERA data which takes into account heavy quark masses and possibly now available next-to-leading order corrections to the virtual photon impact factor with massless quarks. On the level of the $\gamma p \rightarrow V p$ cross-section this would then further require the determination of corresponding NLO corrections for the $\gamma \rightarrow V$ impact factor, *e.g.* using the calculational techniques developed and used in NLO calculations within high energy factorization [43–45].

Acknowledgments

The authors acknowledge support by CONACyT-Mexico grant number CB-2014-241408. We further would like to thank Laurent Favart for pointing out an erroneous H1 data point in an earlier version of this paper.

A Integrals used in the calculation of the impact factor

To determine $N(\mathbf{r}, x)$ from the BFKL gluon density, it is necessary to calculate

$$\int \frac{d^2 \mathbf{k}}{\mathbf{k}^2} \left(1 - e^{i\mathbf{k} \cdot \mathbf{r}}\right) \frac{1}{(\mathbf{k}^2)^{1-\gamma}}. \quad (27)$$

With $\Re\gamma = 1/2$ the individual integrals are not convergent. It is therefore necessary to introduce a regulator $\mathbf{k}^2 > \Lambda$ which will set to zero at the end of the calculation (after cancellation of the divergence in Eq. (27)). We obtain

$$\lim_{\Lambda \rightarrow 0} \int \frac{d^2 \mathbf{k}}{\pi} \frac{e^{i\mathbf{k} \cdot \mathbf{r}}}{(\mathbf{k}^2)^{2-\gamma}} \Theta(\mathbf{k}^2 - \Lambda^2) = \frac{\Gamma(\gamma - 1)}{\Gamma(2 - \gamma)} \left(\frac{\mathbf{r}^2}{4}\right)^{1-\gamma} + \frac{\Lambda^{\gamma-1}}{1 - \gamma}, \quad (28)$$

while

$$\int \frac{d^2 \mathbf{k}}{\pi} \frac{\Theta(\mathbf{k}^2 - \Lambda)}{(\mathbf{k}^2)^{2-\gamma}} = \frac{\Lambda^{\gamma-1}}{1 - \gamma}. \quad (29)$$

and therefore

$$\int \frac{d^2 \mathbf{k}}{\mathbf{k}^2} \left(1 - e^{i\mathbf{k} \cdot \mathbf{r}}\right) \frac{1}{(\mathbf{k}^2)^{1-\gamma}} = -\pi \frac{\Gamma(\gamma - 1)}{\Gamma(2 - \gamma)} \left(\frac{\mathbf{r}^2}{4}\right)^{1-\gamma} = \frac{\pi \Gamma(\gamma) 4^{\gamma-1}}{(1 - \gamma) \Gamma(2 - \gamma) (\mathbf{r}^2)^{\gamma-1}}. \quad (30)$$

In a second step we need to integrate over the dipole size r . With

$$K_0(r\epsilon) = \frac{1}{2} \int_0^\infty \frac{d\lambda}{\lambda} e^{-\lambda\epsilon^2 - \frac{r^2}{4\lambda}}, \quad \frac{r}{\epsilon} K_1(r\epsilon) = \frac{1}{2} \int_0^\infty d\lambda e^{-\lambda\epsilon^2 - \frac{r^2}{4\lambda}}, \quad (31)$$

this can be done using the following integral:

$$\begin{aligned} f(a, b, Q_0^2) &= \int_0^\infty d\lambda \lambda^{a-1} \int \frac{d^2 \mathbf{r}}{\pi} e^{-\lambda\epsilon^2 - \frac{r^2}{4\lambda}} e^{-r^2 Q_0^2} \frac{1}{(\mathbf{r}^2)^b} \\ &= \Gamma(1 - b) \Gamma(1 + a - b) 4^{-a} (Q_0^2)^{b-a-1} U\left(1 + a - b, 1 + a, \frac{\epsilon^2}{4Q_0^2}\right) \end{aligned} \quad (32)$$

where U is a Hypergeometric function of the second kind or Kummer's function.

References

- [1] L. N. Lipatov, Sov. J. Nucl. Phys. **23** (1976) 338, E. A. Kuraev, L. N. Lipatov, V. S. Fadin, Phys. Lett. B **60** (1975) 50, Sov. Phys. JETP **44** (1976) 443, Sov. Phys. JETP **45** (1977) 199. I. I. Balitsky, L. N. Lipatov, Sov. J. Nucl. Phys. **28** (1978) 822.
- [2] V. S. Fadin, L. N. Lipatov, Phys. Lett. B **429** (1998) 127, M. Ciafaloni, G. Camici, Phys. Lett. B **430** (1998) 349.
- [3] M. Misiura [CMS Collaboration], Acta Phys. Polon. B **45**, no. 7, 1543 (2014); B. Ducloué, L. Szymanowski and S. Wallon, Phys. Rev. Lett. **112** (2014) 082003 [arXiv:1309.3229 [hep-ph]]; F. Caporale, D. Y. Ivanov, B. Murdaca and A. Papa, Eur. Phys. J. C **74** (2014) no.10, 3084 Erratum: [Eur. Phys. J. C **75** (2015) no.11, 535] [arXiv:1407.8431 [hep-ph]].

- [4] F. Caporale, G. Chachamis, B. Murdaca and A. Sabio Vera, Phys. Rev. Lett. **116**, no. 1, 012001 (2016) [arXiv:1508.07711 [hep-ph]]; F. Caporale, F. G. Celiberto, G. Chachamis and A. Sabio Vera, Eur. Phys. J. C **76**, no. 3, 165 (2016) [arXiv:1512.03364 [hep-ph]]; F. Caporale, F. G. Celiberto, G. Chachamis, D. G. Gomez and A. Sabio Vera, arXiv:1603.07785 [hep-ph]; arXiv:1606.00574 [hep-ph].
- [5] G. P. Salam, JHEP **9807** (1998) 019 [hep-ph/9806482].
- [6] A. Sabio Vera, Nucl. Phys. B **722** (2005) 65 [hep-ph/0505128].
- [7] M. Hentschinski, A. Sabio Vera and C. Salas, Phys. Rev. Lett. **110** (2013) no.4, 041601 [arXiv:1209.1353 [hep-ph]].
- [8] M. Hentschinski, A. Sabio Vera and C. Salas, Phys. Rev. D **87** (2013) no.7, 076005 [arXiv:1301.5283 [hep-ph]].
- [9] G. Chachamis, M. Deàk, M. Hentschinski, G. Rodrigo and A. Sabio Vera, JHEP **1509**, 123 (2015) [arXiv:1507.05778 [hep-ph]].
- [10] S. P. Jones, A. D. Martin, M. G. Ryskin and T. Teubner, J. Phys. G **41**, 055009 (2014) [arXiv:1312.6795 [hep-ph]].
- [11] S. P. Jones, A. D. Martin, M. G. Ryskin and T. Teubner, JHEP **1311**, 085 (2013) [arXiv:1307.7099].
- [12] V. P. Goncalves, L. A. S. Martins and W. K. Sauter, Eur. Phys. J. C **76** (2016) no.2, 97 [arXiv:1511.00494 [hep-ph]].
- [13] R. Fiore, L. Jenkovszky, V. Libov and M. Machado, Theor. Math. Phys. **182**, no. 1, 141 (2015) [Teor. Mat. Fiz. **182**, no. 1, 171 (2014)] [arXiv:1408.0530 [hep-ph]].
- [14] N. Armesto and A. H. Rezaeian, Phys. Rev. D **90**, no. 5, 054003 (2014) [arXiv:1402.4831 [hep-ph]].
- [15] V. P. Goncalves, B. D. Moreira and F. S. Navarra, Phys. Rev. C **90**, no. 1, 015203 (2014) [arXiv:1405.6977 [hep-ph]].
- [16] V. P. Goncalves, B. D. Moreira and F. S. Navarra, Phys. Lett. B **742**, 172 (2015) [arXiv:1408.1344 [hep-ph]].
- [17] W. Schäfer and A. Szczurek, Phys. Rev. D **76**, 094014 (2007) [arXiv:0705.2887 [hep-ph]]; A. Cisek, W. Schäfer and A. Szczurek, JHEP **1504**, 159 (2015) [arXiv:1405.2253 [hep-ph]].
- [18] M. S. Costa and M. Djuric, Phys. Rev. D **86**, 016009 (2012) [arXiv:1201.1307 [hep-th]]; M. S. Costa, M. Djuri and N. Evans, JHEP **1309** (2013) 084 [arXiv:1307.0009 [hep-ph]].
- [19] V. P. Goncalves and W. K. Sauter, Phys. Rev. D **81**, 074028 (2010) [arXiv:0911.5638 [hep-ph]]; Eur. Phys. J. A **47**, 117 (2011) [arXiv:1004.1952 [hep-ph]].
- [20] J. Kwiecinski, A. D. Martin and A. M. Stasto, Phys. Rev. D **56**, 3991 (1997) [hep-ph/9703445]; A. Bialas, H. Navelet and R. B. Peschanski, Nucl. Phys. B **603**, 218 (2001) [hep-ph/0101179].

- [21] S. J. Brodsky, G. P. Lepage and P. B. Mackenzie, Phys. Rev. D **28** (1983) 228.
- [22] W. Celmaster and R. J. Gonsalves, Phys. Rev. D **20** (1979) 1420.
- [23] S. J. Brodsky, V. S. Fadin, V. T. Kim, L. N. Lipatov and G. B. Pivovarov, JETP Lett. **76** (2002) 249 [Pisma Zh. Eksp. Teor. Fiz. **76** (2002) 306] [hep-ph/0207297]; JETP Lett. **70** (1999) 155 [hep-ph/9901229].
- [24] B. R. Webber, JHEP **9810** (1998) 012 [hep-ph/9805484].
- [25] H. Kowalski, L. Motyka and G. Watt, Phys. Rev. D **74**, 074016 (2006) [hep-ph/0606272].
- [26] B. E. Cox, J. R. Forshaw and R. Sandapen, JHEP **0906**, 034 (2009) [arXiv:0905.0102 [hep-ph]].
- [27] S. J. Brodsky, T. Huang and G. P. Lepage, “The Hadronic Wave Function in Quantum Chromodynamics,” SLAC-PUB-2540.
- [28] J. Nemchik, N. N. Nikolaev and B. G. Zakharov, Phys. Lett. B **341**, 228 (1994) [hep-ph/9405355], J. Nemchik, N. N. Nikolaev, E. Predazzi and B. G. Zakharov, Z. Phys. C **75**, 71 (1997) [hep-ph/9605231], Z. Phys. C **75**, 71 (1997) [hep-ph/9605231].
- [29] K. Kutak and A. M. Stasto, Eur. Phys. J. C **41**, 343 (2005) [hep-ph/0408117].
- [30] S. P. Baranov, Phys. Rev. D **76**, 034021 (2007).
- [31] A. G. Shuvaev, K. J. Golec-Biernat, A. D. Martin and M. G. Ryskin, Phys. Rev. D **60**, 014015 (1999) [hep-ph/9902410].
- [32] S. Chekanov *et al.* [ZEUS Collaboration], Eur. Phys. J. C **24**, 345 (2002) [hep-ex/0201043].
- [33] S. Chekanov *et al.* [ZEUS Collaboration], Nucl. Phys. B **695**, 3 (2004) [hep-ex/0404008].
- [34] C. Alexa *et al.* [H1 Collaboration], Eur. Phys. J. C **73**, no. 6, 2466 (2013) [arXiv:1304.5162 [hep-ex]].
- [35] A. Aktas *et al.* [H1 Collaboration], Eur. Phys. J. C **46**, 585 (2006) [hep-ex/0510016].
- [36] B. B. Abelev *et al.* [ALICE Collaboration], Phys. Rev. Lett. **113**, no. 23, 232504 (2014) [arXiv:1406.7819 [nucl-ex]].
- [37] R. Aaij *et al.* [LHCb Collaboration], J. Phys. G **40**, 045001 (2013) [arXiv:1301.7084 [hep-ex]]; J. Phys. G **41**, 055002 (2014) [arXiv:1401.3288 [hep-ex]].
- [38] C. Adloff *et al.* [H1 Collaboration], Phys. Lett. B **483**, 23 (2000) [hep-ex/0003020].
- [39] J. Breitweg *et al.* [ZEUS Collaboration], Phys. Lett. B **437** (1998) 432 [hep-ex/9807020].
- [40] S. Chekanov *et al.* [ZEUS Collaboration], Phys. Lett. B **680**, 4 (2009) [arXiv:0903.4205 [hep-ex]].
- [41] R. Aaij *et al.* [LHCb Collaboration], JHEP **1509**, 084 (2015) [arXiv:1505.08139 [hep-ex]].

- [42] CMS Collaboration [CMS Collaboration], “Measurement of exclusive Y photoproduction in pPb collisions at $\sqrt{s_{\text{NN}}} = 5.02$ TeV,” CMS-PAS-FSQ-13-009.
- [43] M. Hentschinski and A. Sabio Vera, Phys. Rev. D **85** (2012) 056006 [arXiv:1110.6741 [hep-ph]]; M. Hentschinski, Nucl. Phys. B **859** (2012) 129 [arXiv:1112.4509 [hep-ph]]; G. Chachamis, M. Hentschinski, J. D. Madrigal Martínez and A. Sabio Vera, Nucl. Phys. B **876** (2013) 453 [arXiv:1307.2591 [hep-ph]]; Phys. Rev. D **87** (2013) no.7, 076009 [arXiv:1212.4992]; Nucl. Phys. B **861** (2012) 133 [arXiv:1202.0649 [hep-ph]];
- [44] M. Hentschinski, J. D. Madrigal Martínez, B. Murdaca and A. Sabio Vera, Phys. Lett. B **735** (2014) 168 [arXiv:1404.2937 [hep-ph]]; Nucl. Phys. B **887** (2014) 309 [arXiv:1406.5625 [hep-ph]]; Nucl. Phys. B **889** (2014) 549 [arXiv:1409.6704 [hep-ph]];
- [45] A. Ayala, M. Hentschinski, J. Jalilian-Marian and M. E. Tejeda-Yeomans, arXiv:1604.08526 [hep-ph].